Published in final edited form as:
Dent Mater. 2011 June ; 27(6): 509–519. doi:10.1016/j.dental.2011.01.006.

Control of polymerization shrinkage and stress in nanogel-modified monomer and composite materials

Rafael R. Moraes[1], **Jeffrey W. Garcia**[2], **Matthew D. Barros**[2], **Steven H. Lewis**[2], **Carmem S. Pfeifer**[2], **JianCheng Liu**[3], and **Jeffrey W. Stansbury**[2,3,*]

[1] School of Dentistry, Federal University of Pelotas, RS, Brazil

[2] Department of Craniofacial Biology, University of Colorado Denver School of Dental Medicine, Aurora, CO, USA

[3] Department of Chemical and Biological Engineering, University of Colorado Boulder, Boulder, CO, USA

Abstract

Objectives—This study demonstrates the effects of nano-scale prepolymer particles as additives to model dental monomer and composite formulations.

Methods—Discrete nanogel particles were prepared by solution photopolymerization of isobornyl methacrylate and urethane dimethacrylate in the presence of a chain transfer agent, which also provided a means to attach reactive groups to the prepolymer. Nanogel was added to triethylene glycol dimethacrylate (TEGDMA) in increments between 5 and 40 wt% with resin viscosity, reaction kinetics, shrinkage, mechanical properties, stress and optical properties evaluated. Maximum loading of barium glass filler was determined as a function of nanogel content and composites with varied nanogel content but uniform filler loading were compared in terms of consistency, conversion, shrinkage and mechanical properties.

Results—High conversion, high molecular weight internally crosslinked and cyclized nanogel prepolymer was efficiently prepared and redispersed into TEGDMA with an exponential rise in viscosity accompanying nanogel content. Nanogel addition at any level produced no deleterious effects on reaction kinetics, conversion or mechanical properties, as long as reactive nanogels were used. A reduction in polymerization shrinkage and stress was achieved in proportion to nanogel content. Even at high nanogel concentrations, the maximum loading of glass filler was only marginally reduced relative to the control and high strength composite materials with low shrinkage were obtained.

Significance—The use of reactive nanogels offers a versatile platform from which resin and composite handling properties can be adjusted while the polymerization shrinkage and stress development that challenge the adhesive bonding of dental restoratives are controllably reduced.

[*]Corresponding author contact information: Jeffrey W. Stansbury, University of Colorado Denver, MS 8310, 12800 E 19th Ave, Rm 2104, Aurora, CO 80045, USA, jeffrey.stansbury@ucdenver.edu.

Introduction

Extensive research work has been conducted regarding materials and light-curing methods designed to reduce the overall stress state in dental composites during constrained polymerization. This has included the development of a wide variety of novel monomers that provide reduced shrinkage compared with conventional dimethacrylates [1, 2], use of compliant liners in dental restorations [3, 4], and varied photo-activation protocols that alter reaction kinetics [5–7]. Polymerization stress is related to polymer modulus and polymerization shrinkage [8] while polymerization shrinkage is dependent on conversion and initial reactive group concentration [9, 10]. Therefore, a reduction in polymerization shrinkage while maintaining fixed modulus and conversion in the final polymer is expected to provide a proportional reduction in polymerization stress. In this investigation, high molecular weight polymeric nanoparticles (nanogels) are used as a swellable, potentially reactive additive in a secondary monomer with the goal to reduce the overall reactive group concentration and thereby reduce polymerization shrinkage and stress without compromise to other critical polymer properties.

Nanogels are internally crosslinked and cyclized single or multi-chain polymeric particles typically well below micrometer size. These materials have attracted substantial interest and have been prepared from very diverse monomer compositions by a number of synthetic routes designed to maintain discrete nanoparticle formation without macrogelation [11–16]. Practical applications of nanogels include drug delivery, biosensing, microreactors, modifiers for coatings and polymer composites [17–20].

The use of prepolymerized particles in dental composites is obviously not novel since microfilled composites use an “organic filler” approach, whereby inorganic filler and resin are cured, crushed and added to monomer and filler [21] to produce the final composite material. However, the particle size of the pulverized prepolymer is relatively large and the overall amount of filler that can be incorporated into these composites is limited, which results in higher coefficients of thermal expansion and water sorption as well as lower elastic moduli compared with conventional dental composites [22, 23]. In contrast, the use of nanogel prepolymer in composite applications may present a more versatile approach that allows a greater amount of inorganic filler to be incorporated due to the nanoscopic size of these prepolymer particles. Because the great majority of polymerization involving nanogels is performed prior to its introduction into a secondary monomer, the volumetric shrinkage in nanogel-modified materials is expected to scale inversely with nanogel loading. Nanogels bearing reactive sites, which may include both internal and surface-situated functional groups, have been prepared previously [14, 24].

There are a number of examples of hyperbranched or dendritic macromers applied as components of dental restorative materials [25–28]. The hyperbranched monomers used are generally well characterized structurally, but fairly low in molecular weight with a high degree of methacrylate group functionalization. Polymeric fibers produced by electrospinning processes represent another means to incorporate prepolymer into dental composites [29]. There are no literature reports regarding the use of nanogel particles in dental polymers. The current study seeks to demonstrate a simple method to prepare reactive nanogels as well as the comprehensive evaluation of a model nanogel as an additive in triethylene glycol dimethacrylate (TEGDMA) as a model monomer matrix. The incorporation of inorganic filler in the nanogel-modified monomer is also examined to provide further relevance to dimethacrylate dental composite materials. This approach may offer a unique ability to controllably modify polymerization shrinkage, modulus and stress depending on the nanogel size, structure and fraction incorporated. The hypothesis tested is that substantial nanogel contents can be accommodated in both unfilled and filled resin

formulations to reduce polymerization shrinkage and stress without detrimental impact to other critical material properties.

Materials and Methods

Nanogel synthesis

Copolymer nanogels were synthesized by a batch process using a 70:30 molar ratio of isobornyl methacrylate (IBMA; Sigma-Aldrich Co., St. Louis, MO, USA) and urethane dimethacrylate (UDMA; Esstech, Essington, PA, USA), respectively. Free-radical polymerization was carried out in solution using a four-fold excess of toluene (relative to monomer mass) as a solvent. Bis(2,4,6-trimethylbenzoyl)-phenylphosphine oxide (BAPO, Irgacure 819; Ciba Specialty Chemicals, Basel, Switzerland) at 2.5 wt% was used as the photoinitiator. 2-Mercaptoethanol (ME; Sigma-Aldrich, 15 mol% relative to monomers) was included as a chain transfer agent to aid in the prevention of macrogelation as well as to provide sites for post-polymerization refunctionalization with methacrylate groups. Room temperature (23 °C) light-activation of the reactant mixture was conducted with an output irradiance of 2500 mW/cm^2 between 320 and 500 nm (Novacure; EXFO, Mississauga, Ontario, Canada) for approximately 2 h during which time, methacrylate conversion of greater than 90 % was achieved (based on C=C peak area at 1637 cm^{-1} relative to the C=O absorbance at 1720 cm^{-1}; includes both pendant vinyl groups and unreacted free monomer) as determined from the initial and final mid-infrared spectra (Nicolet 6700, Thermo Scientific, West Palm Beach, FL, USA). A foil-wrapped 100 mL round-bottom flask was used as the photoreactor with monomer batch sizes of approximately 10 g. Nanogel was precipitated from the clear reaction mixture by dropwise addition into an excess of hexane. The precipitate was filtered and the residual solvent was removed under reduced pressure to obtain the nanogel as a dry powder in approximately 85 % yield. In order to obtain reactive, polymerizable nanogels, half of the isolated nanogel was added to a four-fold excess of methylene chloride to give a clear dispersion, which was mixed with a slight excess of 2-isocyanoethyl methacrylate (IEM; Sigma-Aldrich) (equimolar based on the original ME content) and stirred for 6 h in the presence of a trace amount of dibutyltin dilaurate (Sigma-Aldrich) as catalyst. The polymer precipitation method was repeated to isolate the methacrylate-functionalized reactive nanogel. The structures of the reagents used are shown in Figure 1.

Nanogel particle characterization

The polymeric nanogels were characterized by triple detector (differential refractive index, viscosity, light scattering) gel permeation chromatography (GPC; Viscotek, Houston, TX, USA) in tetrahydrofuran using a series of four columns spanning molecular weights of 10^4 to 10^7 with absolute molecular weight based on right/low angle light scattering detection calibrated with a 65 kDa poly(methyl methacrylate) standard. As a control, IBMA was homopolymerized in solution with chain transfer agent under the same conditions used to prepare the nanogel. The glass transition temperature (T_g) of the dry nanogel powder (n = 2) was determined with a dynamic mechanical analyzer (DMA; Perkin Elmer 8000, Waltham, MA, USA) by sandwiching 10 mg of nanogel in a thin metallic pocket that was then subjected to single cantilever cyclic displacement of 50 μm at 1 Hz. The nanogel was heated to 180 °C with tan δ data collected as the sample was cooled to −50 °C at 2 °C/min in air. The density of the dry nanogel powder was determined using a helium-purged pycnometer (MVP-60C; Quantachrome Instruments, Boynton Beach, FL, USA).

Formulation of resins and composites

TEGDMA (Esstech) was used as a matrix monomer to be loaded with nanogel. The nanogel was loaded at 5, 10, 20, 30 or 40 wt%, for both reactive and non-reactive particles, with

unfilled TEGDMA used as a control. Corresponding dual-filled resin composites were obtained by progressively loading the reactive nanogel-modified TEGDMA samples with the maximum capacity of barium borosilicate glass particles (0.4 μm average diameter) treated with 5 wt% of γ-methacryloxypropyltrimethoxysilane; Esstech) that could be incorporated homogeneously, based on visual inspection coupled with incremental filler addition (single determinations), using a centrifugal mixer (SpeedMixer DAC150; FlackTek, Landrum, SC, USA). In addition, the same TEGDMA/reactive nanogel series was loaded with a uniform barium glass filler content of 70 wt%. In order to render all these materials photo-curable with either UV or visible irradiation, 0.2 wt% of BAPO (relative to the resin content) was included in each mixture.

Viscosity and consistency

Viscosity measurements of the nanogel-modified TEGDMA materials were performed using a cone-plate digital viscometer (CAP2000+; Brookfield, Middleboro, MA, USA). A defined volume of the control and nanogel-modified monomer was tested at 25 °C under the following conditions: 200 rpm, 1 Hz, and a run time of 30 s. Consistency of the 70 wt% barium glass filled composite materials was measured on a universal testing machine (858 Mini Bionix; MTS Systems, Eden Prairie, MN, USA) at 23 °C. A defined volume of the various composite paste samples was placed into a glass cylinder (20 mm high × 10 mm diameter) and compacted such that the material completely filled the bottom of the container to a uniform depth. A 7.5 mm diameter brass cylindrical plunger was lowered into the paste at a rate of 5 mm/min until the tip of the plunger was 1 mm from the bottom of the well. The load-extension data were collected and the peak force was recorded. Three measurements were carried out for each material.

Photopolymerization reaction kinetics and conversion

Real-time monitoring of the polymerization kinetics was carried out using near-infrared (NIR) spectroscopy. The area of the methacrylate $=CH_2$ peak (6163 cm^{-1}) was recorded with 4 scans per spectrum at 4 wave-number resolution. To monitor the change of the carbon-carbon double bond concentration during polymerization, a series run collected the predefined peak area as a function of time. Samples (n = 3) were irradiated for 5 min with the filtered 320–500 nm output of a mercury arc lamp (Acticure 4000; EFOS) at an incident irradiance of 50 mW/cm^2. Conversion versus time data were plotted and Hill's 4 parameter non-linear regression was used for curve fitting. As the regression coefficient was greater than 0.99 for all curves, the rate of polymerization (R_p) was calculated using these data-fitted plots.

Volumetric shrinkage

A constant volume of each resin was placed onto an aluminum disc in a non-contact linear variable differential transducer-based linometer (Academic Center for Dentistry Amsterdam, The Netherlands). The material was covered with a glass slide, which was adjusted to produce a specimen disc (approximately 1 × 6 mm). The displacement caused by linear shrinkage during photopolymerization was measured, and converted to the corresponding volumetric shrinkage. Shrinkage measurements of the dual-filled composite materials were carried out using a mercury dilatometer (Paffenbarger Research Center, American Dental Association, Gaithersburg, MD, USA) with integrated temperature correction. Both the resin and composite specimens were irradiated for 40 s with 400–500 nm light at an irradiance of 600 mW/cm^2 using a halogen dental curing unit (Optilux 501; Demetron Kerr, Orange, CA, USA). The dynamic shrinkage data was recorded during and extending beyond the irradiation interval for a total period of 10 min (resins) or 60 min (composites). Three replicates were carried out for each material.

Polymerization stress

The dynamic shrinkage stress was evaluated for selected nanogel-modified TEGDMA formulations (0, 20 and 40 wt% reactive nanogel) with a tensometer (Paffenbarger Research Center, American Dental Association) as previously described [30]. A 1 × 6 mm specimen size was used with photocuring provided by continuous irradiation by the Acticure mercury arc lamp at 800 mW/cm^2 for 10 min. The simultaneous real-time NIR based conversion data during polymerization was collected in direct transmission mode via fiber optic cables (1 mm diameter single fiber).

Mechanical strength characterization

Flexural strength tests for all materials were performed using bar specimens (n = 5) with dimensions of 15 × 2 × 2 mm photopolymerized between glass slides in an elastomer mold by exposure to halogen-based visible light at 600 mW/cm^2 for 3 min on each side. After 24 h storage in the dark under ambient conditions, the flexural strength (σ) and flexural modulus (E_f) were obtained in three-point bending on the MTS testing machine using a span of 10 mm and a cross-head speed of 1 mm/min.

Optical properties

The refractive indices of the resins were measured using an Abbe refractometer (model NAR-27; ATAGO Co. Ltd., Tokyo, Japan), at 23 °C with measurement accuracy of ± 0.0002. Variations in optical density of the nanogel-loaded monomer and polymer formulations compared with the unmodified TEGDMA monomer and polymer were determined by measurement of the relative transmitted intensities of 758 nm light through specimens (n = 3) in a 1 cm pathlength cuvette at room temperature.

Statistical analysis

Data from each evaluation were submitted to One-Way Analysis of Variance (for composites, non-reactive and reactive resins individually), followed by Tukey's as *post-hoc* test. Comparisons between analogous nanogel concentrations in the reactive and non-reactive subsets were performed by paired t-tests. Regressions analyses were carried out to investigate the relationship between nanogel fraction and shrinkage. All analyses were performed at a global level of significance of 95 %.

Results and Discussion

Nanogel synthesis

The effects of variations in the selection and relative concentrations of monomers, chain transfer agents, initiators and solvent, as well as the in the choice of reaction conditions, on nanogel structure and properties will be addressed in a separate report. Here, we have elected to highlight one basic nanogel material, in both reactive and non-reactive forms, as an additive in TEGDMA monomer and in analogous composite formulations prepared with barium glass filler. A UV/visible light-induced solution polymerization was used to generate the nanogel material with high efficiency. Under the conditions used here, a chain transfer agent is not necessary to avoid macrogelation, even at high conversion and with the relatively high concentration (30 mol%) of UDMA used as the crosslinker. However, inclusion of an alkyl thiol limits polymer chain length and introduces a relatively high concentration of chain ends, many of which are subsequently appended with a reactive urethane methacrylate group from the addition of IEM to the hydroxyl group associated with ME located nearly exclusively at chain ends based on the chain transfer process. The mid-IR spectra obtained from the initial and final nanogel reaction mixture indicates a conversion of 92 %, which increases to approximately 95 % conversion for the precipitated nanogel where

the residual methacrylate represents the limited number of pendant double bonds within the nanogel. The mid-IR analysis is also useful to follow the addition of IEM to the thiol-terminated chain ends. The location of methacrylate groups on mobile and readily accessible chain ends may make these reactive sites more effective in copolymerization with the matrix monomer than the pendant vinyls remaining from the initial nanogel synthesis. The consumption of alkyl thiol and methacrylate monomer in chain transfer dominated network photopolymerizations has been described previously [31, 32]. Based on the thiol absorbance at 2585 cm^{-1} in the mid-IR spectra, it appears that only about 25 % of the ME is incorporated into the nanogel; however, the IR also shows that the nanogel precipitation step effectively removes the excess thiol and there is no thiol odor associated with the precipitated nanogel. Our prior work indicated the mechanical property advantages associated with the use of reactive nanogels, rather than the essentially inert initially prepared nanogels, to modify dental resins [33].

Particle characterization

Triple detection GPC analysis of the nanogels provides not only molecular weight and polydispersity data, but also information on molecular structure and size based on the viscosity and light scattering detection capabilities along with the standard refractive index mode of detection. The roughly spherical or globular structure of the nanogel is confirmed by the Mark-Houwink α value of 0.37 as opposed to a typical value of approximately 0.7 associated with a random coil linear polymer structures [11]. The IBMA solution homopolymerization in the presence of ME produced polymer with a weight average molecular weight (M_w) of 5,600 Da and a polydispersity of 1.3. With UDMA included in the polymerization, nanogel is formed with a M_w of 1.02×10^6 Da, a polydispersity of 5.8 and an average hydrodynamic radius of 8.6 nm with an upper limit of 30–40 nm. By application of the IBMA homopolymer as a linear reference and assuming a trifunctional branching model in the Zimm-Stockmayer expression [34], the GPC-based calculated weight average branching number per nanogel is approximately 60, which indicates a highly branched and cyclized macromolecular structure.

The thermal scan of the bulk nanogel powder by dynamic mechanical analysis provided a T_g of 92.9 ± 0.8 °C and a tan δ peak width at half height of 32 ± 4 °C. As a control, a commercial poly(methyl methacrylate) (PMMA; Sigma-Aldrich; 120,000 Da) powder was evaluated in the DMA under the same conditions with the resulting T_g value of 108.8 ± 0.7 °C in reasonable agreement with the PMMA literature value of 105 °C [35]. The nanogel T_g is significantly lower than that of IBMA homopolymer (145.3 ± 2.2 °C with a half-height tan δ peak width of 54.1 ± 0.4 °C) probably as a result of the relatively high concentration of chain ends associated with the highly branched but open nanogel structure; however, the nanogel Tg is significantly higher than that of TEGDMA homopolymer photocured at room temperature. The density of the collapsed nanogel as an aggregated dry powder was approximately 1.14 g/cm^3. This value is bracketed by the densities of TEGDMA monomer and homopolymer (70 % conversion) at 1.07 and 1.18 g/cm^3, respectively. The barium glass filler used in the composite samples had a density of 3.04 g/cm^3 and therefore, the 70 wt% inorganic filler loading accounts for volume fractions of 45.1 % in the TEGDMA control and 45.7 % in the experimental material at the 40 wt% nanogel loading level (assuming additive densities within the resin phase).

Monomer viscosity, filler loading capacity and composite consistency

The effect of low nanogel additive contents on TEGDMA viscosity (Table 1 and Figure 2) is minimal as is typically observed for globular/spherical hyperbranched or dendritic polymeric additives [36]. While the difference was small, the reactive nanogel bearing urethane methacrylate functionality consistently yielded lower viscosity TEGDMA

compositions compared with the same mass fraction of the inert nanogel with the stronger hydrogen bonding hydroxyl functionality [37]. Irrespective of whether reactive or non-reactive nanogels were employed, as the nanogel loading levels extend beyond 20 wt%, the percolation threshold is approached where particle-particle interactions begin to dominate over resin-particle interactions. A calculation based on monodisperse 10 nm nonporous particles predicts approximately 5 nm inter-particle spacing at only a 20 vol% loading level [38]. Here, the nanogel particles are significantly swollen with monomer, which leads to an increased effective volume fraction compared with the calculation based simply on mass and density considerations. The exponential rise in viscosity at high nanogel content is an indication that at 40 wt% nanogel, the matrix phase is approaching a continuous interphase rather than some combination of bulk TEGDMA and the interfacial regions around the nanogels. However, as shown in Table 1, despite the presumptive limitation of a bulk TEGDMA phase at high nanogel concentrations, the maximum loading of inorganic filler was only modestly reduced compared with the TEGDMA control.

A comparison of the nanogel loading effects on consistency of the dual-filled composites with uniform inorganic filler content (70 wt% barium glass) is shown in Figure 3 with the respective force/displacement slopes provided in Table 1. Only slight differences were detected for the consistency profiles of the dual-filled composites containing 5 or 10 wt% of nanogel compared with the unmodified composite. At 20 wt% nanogel in the resin phase of the composite, a modest increase is noted in the penetration resistance, which agrees with the onset of the viscosity rise in unfilled monomer. The dual-filled composites containing 30 and 40 wt% of nanogel presented substantial increases in the stress-strain profiles during the consistency test but these heavy body pastes still offer manageable handling properties, comparable to commercial microhybrid dental composites.

Polymerization kinetics

The dry nanogel powder can be redispersed into solvent or monomer of an appropriate solubility parameter to give stable colloidal suspensions. Since the nanogel is formed in a solution polymerization process, the polymeric particles are significantly swollen by monomer. This means an effective volume fraction of swollen nanogel rather than a simple calculated volume fraction may be more appropriately used in evaluations of nanogel-modified resin and composite properties. However, the discussion here will be restricted to nanogel contents based only on simple weight fractions, which is appropriate since the density difference between the matrix monomer and the monomer-swollen nanogel is minimal meaning near-equivalence of weight and volume fractions. Photopolymerization kinetics plots and the accompanying rate plots are shown in Figures 4 and 5, respectively. The reaction kinetics profile of the TEGDMA control was similar to all the nanogel-modified resins, irrespective of the nanogel concentration and whether reactive or non-reactive nanoparticles were used. In general, the addition of nanogel caused an earlier onset of autoacceleration, which can be linked to the mobility restricted environment for TEGDMA monomer in and around the nanogel particles. Particularly for the reactive nanogels, the onset of autodecceleration occurred earlier and at lower conversion compared with the control. No appreciable differences in final conversion values were observed with values reaching approximately 70 % for all materials. The addition of 10 wt% or 20 wt% and higher of nanogel to TEGDMA decreased the maximum rate of polymerization (R_p^{max}) as might be expected since the presence of nanogel limits the potential exotherm. However, the added nanogel promoted somewhat higher reaction rates in the vitrified state, which may be a consequence of the lower crosslink density contributed by the nanogel compared with TEGDMA homopolymer. Within the series of composite materials with a standardized 70 wt% barium glass filler and varying nanogel content, the final limiting conversion attained was also unaffected by the nanogel loading.

Volumetric shrinkage

The addition of either reactive or non-reactive nanogels decreased TEGDMA polymerization shrinkage essentially in direct proportion to the increasing nanogel fraction (Table 2). As expected based on the similarities in the reaction kinetic profiles, the shrinkage kinetics are also consistent regardless of the nanogel content (Figure 6). The addition of 40 wt% of reactive and non-reactive nanogels to TEGDMA decreased polymerization shrinkage by 37 and 43 %, respectively. Conversion assessment on the actual shrinkage disc specimens confirms that the reduction in shrinkage associated with the nanogel addition is not related to any differences in final conversion. No significant differences in shrinkage were apparent between reactive and non-reactive prepolymer particles. In the dual-filled composite materials, 40 wt% of nanogel in the resin phase accounts for 12 wt% or approximately 21 vol% of the overall composite material and provides a 24 % reduction in volumetric shrinkage compared with the TEGDMA composite control. To provide an additional, more practical demonstration, 40 wt% of the reactive nanogel was dispersed into the combination of ethoxylated bisphenol A dimethacrylate, UDMA and TEGDMA (50:30:20 mass ratio) to yield a clear, fluid resin with a volumetric polymerization shrinkage of 4.28 ± 0.3 % compared with 6.69 ± 0.1 % for the unmodified control at equivalent conversion. This 36 % reduction in shrinkage indicates that the beneficial effects of nanogel additives are generic in nature. It should be noted that valid comparisons can be drawn for properties within a given test but since different specimen geometries, curing light sources and photopolymerization conditions were used throughout this study, the results obtained in different tests may not correlate directly.

Mechanical characterization

Results for flexural strength and modulus (Table 3) clearly demonstrate that physical entanglement between the matrix and nanogel is not sufficient to achieve a mechanically sound polymer network despite good conversion. Flexural strength is essentially unaffected at non-reactive nanogel concentrations up to 10 wt%, which based on the viscosity results, corresponds to isolated nanogel domains within the matrix. However, as nanogel confluence is approached at higher loading levels, the ultimate strength, but not modulus, drops dramatically. In contrast, the limited placement of polymerizable methacrylate groups at readily accessible chain ends throughout the nanogel structure, converts the prepolymer to a macromolecular monomer (macromer) and even the highest nanogel loading levels present no reduction in either polymer modulus or flexural strength. The incorporation of reactive nanogel at any level into the 70 wt% barium glass-filled materials contributed a similar neutral effect to the mechanical performance of these dual-filled composites, which indicates that effective covalent attachment is maintained between the filler and the nanogel-modified polymeric matrix.

Polymerization stress

In direct dental restoratives, which necessarily involve bonded interfaces, the stress developed during polymerization is a more critical concern than the extent of shrinkage that occurs in an ideal, non-bonded state. Therefore, it is practically important to demonstrate that the addition of nanogel not only reduces volumetric shrinkage but also the shrinkage stress. The incorporation of 20 or 40 wt% reactive nanogel to TEGDMA monomer yielded materials with final stress level decreases of 26 or 45 % respectively, compared with the control (Figure 7). As previously shown, this stress reduction was achieved without compromise in either conversion or modulus of the resulting polymers. The simultaneous measurement of both real-time conversion and stress development demonstrated a delay to higher conversion for the onset of vitrification in the nanogel-modified compositions (data not shown here). This behavior may be indicative of a higher initial polymerization reaction rate in and around the nanogel particles as noted from the reaction kinetics data. Faster

polymerization and property development within the spatially resolved nanogel particles effectively would produce delayed modulus and vitrification since these bulk properties would be dominated by the slower developing continuous matrix phase.

Optical properties

The refractive index of the TEGDMA/nanogel formulations progressively increased with increasing nanogel fraction. The increase was slightly greater with the non-reactive nanogel particles. Based on the extrapolated linear regression analyses, the refractive indices of the reactive and non-reactive particles were calculated to be 1.5087 and 1.5101, respectively ($R^2 \geq 0.97$, $P < 0.001$). While the nanogel here was not developed with optical properties in mind, it is apparent that nanogels could be designed to significantly raise or lower the matrix phase refractive index in composite materials as a means to adjust overall translucency based on the overall resin-filler refractive index mismatch. The addition of nanogel did have a modest effect in the optical transparency of TEGDMA in both the monomeric and polymeric states. For the unaltered TEGDMA controls, a 13.7% reduction in 758 nm light transmission efficiency was noted for the homopolymer compared with TEGDMA monomer. This may be related to the well known heterogeneity in terms of crosslink density of dimethacrylate polymer networks [39, 40] as well as the potential formation of microvoids and defects within the glassy polymer.

A modest increase in optical density is associated with the nanogel additive relative to the baseline state of TEGDMA either as monomer or polymer (Table 4), but there is no evidence of any phase separation during polymerization that is often encountered with prepolymer addition to monomer. In terms of practical concerns, a slight haziness is evident in the nanogel-modified monomer and polymer samples with little additional effect at 40 wt % nanogel loading compared with 20 wt% (Figure 8). The original nanogel suspensions (at approximately 25 wt% nanogel) prior to isolation by precipitation are essentially transparent as demonstrated by a 99.0 ± 0.3 % relative light transmission efficiency compared with pure toluene. This would be expected for well dispersed polymeric particles with maximum hydrodynamic radii in the range of approximately 40 nm. Following precipitation and evaporation of residual solvent, the redispersion of 25 wt% nanogel into solvent, based on simple room temperature mixing, yields a relative light transmission of 93.9 ± 0.4 % compared with solvent alone. There are a variety of approaches that may allow heavily nanogel-loaded, optically clear monomers and polymers to be prepared but even without efforts to optimize the optical properties here, optical quality at even the highest nanogel content appears quite acceptable for dental materials applications.

Conclusion

Nanogel prepolymer additives were incorporated into a dimethacrylate monomer in substantial quantities without significant effect to reaction kinetics or final conversion attained during photopolymerization. At moderate concentrations of nanogel, monomer viscosity is only modestly increased while high nanogel contents raise monomer viscosity and composite paste consistency dramatically. The relatively high glass transition temperature nanogel used here did not change the modulus of the polymers but the use of reactive nanogels was critical to maintain the flexural strength performance. Most importantly, the introduction of nanogel prepolymer particles was demonstrated to effectively reduce polymerization shrinkage and stress in what is considered to be a broadly generic approach that can also be used to alter resin phase refractive index and still permit high levels of inorganic filler loading in dental composite restorative materials.

Acknowledgments

This work was supported by NIH/NIDCR R21-DE018354 and RC1-DE020480 as well as Septodont. Support for RRM was provided by CAPES/Brazil (protocol 4511/07-7). The TEGDMA and UDMA monomers as well as the glass filler used were generously donated by Esstech.

References

1. Atai M, Ahmadi M, Babanzadeh S, Watts DC. Synthesis, characterization, shrinkage and curing kinetics of a new low-shrinkage urethane dimethacrylate monomer for dental applications. Dent Mater. 2007; 23:1030–41. [PubMed: 17493674]
2. Stansbury JW, Dickens B, Liu DW. Preparation and characterization of cyclopolymerizable resin formulations. J Dent Res. 1995; 74:1110–5. [PubMed: 7782542]
3. Alomari QD, Reinhardt JW, Boyer DB. Effect of liners on cusp deflection and gap formation in composite restorations. Oper Dent. 2001; 26:406–11. [PubMed: 11504442]
4. Alonso RCB, Cunha LG, Correr GM, De Goes MF, Correr-Sobrinho L, Puppin-Rontani RM, Sinhoreti MAC. Association of photoactivation methods and low modulus liners on marginal adaptation of composite restorations. Acta Odont Scand. 2004; 62:298–304. [PubMed: 15848972]
5. Brandt WC, de Moraes RR, Correr L, Sinhoreti MAC, Consani S. Effect of different photo-activation methods on push out force, hardness and cross-link density of resin composite restorations. Dent Mater. 2008; 24:846–50. [PubMed: 18045677]
6. Sakaguchi RL, Berge HX. Reduced light energy density decreases post-gel contraction while maintaining degree of conversion in composites. J Dent. 1998; 26:695–700. [PubMed: 9793292]
7. Sakaguchi RL, Wiltbank BD, Murchison CF. Contraction force rate of polymer composites is linearly correlated with irradiance. Dent Mater. 2004; 20:402–7. [PubMed: 15019457]
8. Braga RR, Ferracane JL. Alternatives in polymerization contraction stress management. Crit Rev Oral Biol Med. 2004; 15:176–84. [PubMed: 15187035]
9. Dewaele M, Truffier-Boutry D, Devaux J, Leloup G. Volume contraction in photocured dental resins: The shrinkage-conversion relationship revisited. Dent Mater. 2006; 22:359–65. [PubMed: 16143380]
10. Stansbury JW, Trujillo-Lemon M, Lu H, Ding X, Lin Y, Ge J. Conversion-dependent shrinkage stress and strain in dental resins and composites. Dent Mater. 2005; 21:56–67. [PubMed: 15681003]
11. Funke W, Okay O, Joos-Muller B. Microgels: Intramolecularly crosslinked macromolecules with a globular structure. Microencapsulation - Microgels - Iniferters. 1998:139–234.
12. Graham NB, Cameron A. Nanogels and microgels: The new polymeric materials playground. Pure Appl Chem. 1998; 70:1271–5.
13. Rouzeau S, Mechin F, Pascault JP, Magny B. Criteria for the preparation of cross-linked poly(meth)acrylate microparticles by solution free radical polymerization. Eur Polym J. 2007; 43:4398–414.
14. Szaloki M, Skribanek R, Dudas Z, JFH, Hegedus C, Borbely J. Preparation of reactive polymeric nanoparticles (RPNPs). Colloid Polym Sci. 2008; 286:435–44.
15. Dvorakova G, Biffis A. Room temperature preparation of highly crosslinked microgels. Polym Bull. 2010; 64:107–14.
16. Isaure F, Cormack PAG, Sherrington DC. Facile synthesis of branched poly(methyl methacrylate)s. J Mater Chem. 2003; 13:2701–10.
17. Ballauff M, Lu Y. “Smart” nanoparticles: Preparation, characterization and applications. Polymer. 2007; 48:1815–23.
18. Fernandez-Barbero A, Suarez IJ, Sierra-Martin B, Fernandez-Nieves A, de las Nieves FJ, Marquez M, Rubio-Retama J, Lopez-Cabarcos E. Gels and microgels for nanotechnological applications. Adv Colloid Interface Sci. 2009; 147–48:88–108.
19. Oh JK. Engineering of nanometer-sized cross-linked hydrogels for biomedical applications. Can J Chem-Rev Can Chim. 2010; 88:173–84.

20. Siegel RA, Gu YD, Lei M, Baldi A, Nuxoll EE, Ziaie B. Hard and soft micro- and nanofabrication: An integrated approach to hydrogel-based biosensing and drug delivery. J Control Release. 2010; 141:303–13. [PubMed: 20036310]
21. Mannerberg F. Isosit, a new material for restoration of anterior teeth. Quintessence Int Dent Dig. 1977; 8:23–32. [PubMed: 275923]
22. Kim KH, Park JH, Imai Y, Kishi T. Fracture-toughness and acoustic-emission behavior of dental composite resins. Eng Fract Mech. 1991; 40:811–9.
23. Papadogianis Y, Boyer DB, Lakes RS. Creep of conventional and microfilled dental composites. J Biomed Mater Res. 1984; 18:15–24. [PubMed: 6230361]
24. Uveges A, Szaloki M, Hartmann JF, Hegedus C, Borbely J. Synthesis of polymeric nanoparticles by cross-linking copolymerization. Macromolecules. 2008; 41:1223–8.
25. Dodiuk-Kenig H, Lizenboim K, Eppelbaum I, Zalsman B, Kenig S. The effect of hyper-branched polymers on the properties of dental composites and adhesives. J Adhes Sci Tech. 2004; 18:1723–37.
26. Paul NM, Bader SJ, Schricker SR, Parquette JR. 2,3-Branching benzyl ether dendrimers for the enhancement of dental composites. React Funct Polym. 2006; 66:1684–95.
27. Viljanen EK, Lassila LVJ, Skrifvars M, Vallittu PK. Degree of conversion and flexural properties of a dendrimer/methyl methacrylate copolymer: design of experiments and statistical screening. Dent Mater. 2005; 21:172–7. [PubMed: 15681016]
28. Wan QC, Schricker SR, Culbertson BM. Methacryloyl derivitized hyperbranched polyester. 2. Photo-polymerization and properties for dental resin systems. J Macromol Sci A. 2000; 37:1317–31.
29. Tian M, Gao Y, Liu Y, Liao YL, Hedin NE, Fong H. Fabrication and evaluation of Bis-GMA/TEGDMA dental resins/composites containing nano fibrillar silicate. Dent Mater. 2008; 24:235–43. [PubMed: 17572485]
30. Lu H, Stansbury JW, Dickens SH, Eichmiller FC, Bowman CN. Probing the origins and control of shrinkage stress in dental resin composites. II. Novel method of simultaneous measurement of polymerization shrinkage stress and conversion. J Biomed Mater Res B. 2004; 71B:206–13.
31. Lecamp L, Houllier F, Youssef B, Bunel C. Photoinitiated cross-linking of a thiol-methacrylate system. Polymer. 2001; 42:2727–36.
32. Lee TY, Smith Z, Reddy SK, Cramer NB, Bowman CN. Thiol-allyl ether-methacrylate ternary systems: Polymerization mechanism. Macromolecules. 2007; 40:1466–72.
33. Stansbury JW, Trujillo-Lemon M, Ding X. Controlled preparation of nanogel particles and their use as macromonomers. Am Chem Soc, Polym Prepr. 2006; 47(2):825–6.
34. Striegel, AM.; Yau, WW.; Kirkland, JJ.; Bly, DD. Modern size-exclusion liquid chromatography: Practice of gel permeation and gel filtration chromatography. 2. Hoboken: Wiley; 2009.
35. Odian, G. Principles of polymerization. 4. New York: Wiley; 2004.
36. Jikei M, Kakimoto M. Hyperbranched polymers: A promising new class of materials. Prog Polym Sci. 2001; 26:1233–85.
37. Lemon MT, Jones MS, Stansbury JW. Hydrogen bonding interactions in methacrylate monomers and polymers. Journal of Biomedical Materials Research: Part A. 2007; 83A:734–746. [PubMed: 17559132]
38. Hao T, Riman RE. Calculation of interparticle spacing in colloidal systems. Journal of Colloid and Interface Science. 2006; 297:374–377. [PubMed: 16515794]
39. Rey L, Galy J, Sautereau H. Reaction kinetics and morphological changes during isothermal cure of vinyl/dimethacrylate networks. Macromolecules. 2000; 33:6780–6786.
40. Richter S. Recent gelation studies on irreversible and reversible systems with dynamic light scattering and rheology – A concise summary. Macromolecular Chemistry and Physics. 2007; 208:1495–1502.

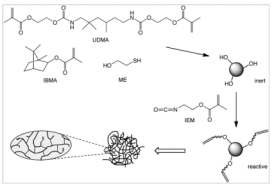

Figure 1.
Structures of monomers and reagents used in the study. High conversion, essentially inert nanogel particles consisting of highly interconnected, relatively short individual polymer chains with branch points at nearly every other monomer unit on average are formed in the first step. Many of the chain ends are hydroxyl-terminated due to the chain transfer process and this allows a route for reintroduction of methacrylate groups to yield reactive nanogels.

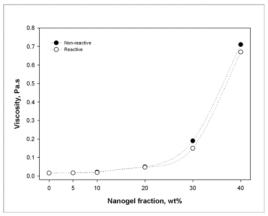

Figure 2.
Nanogel loading effect on TEGDMA viscosity.

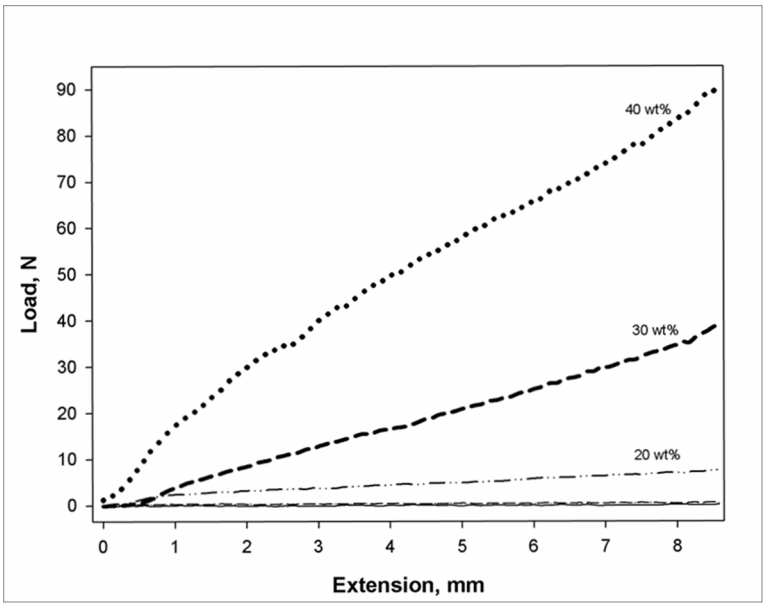

Figure 3.
Composite paste consistency profiles for TEGDMA-based materials containing 70 wt% barium glass and varied amounts of reactive nanogel in the resin phase. The stress-strain plots are the result of the penetration resistance to a cylindrical stylus advanced into the composite paste at 5 mm/min. The 0, 5 and 10 wt% nanogel data are virtually indistinguishable.

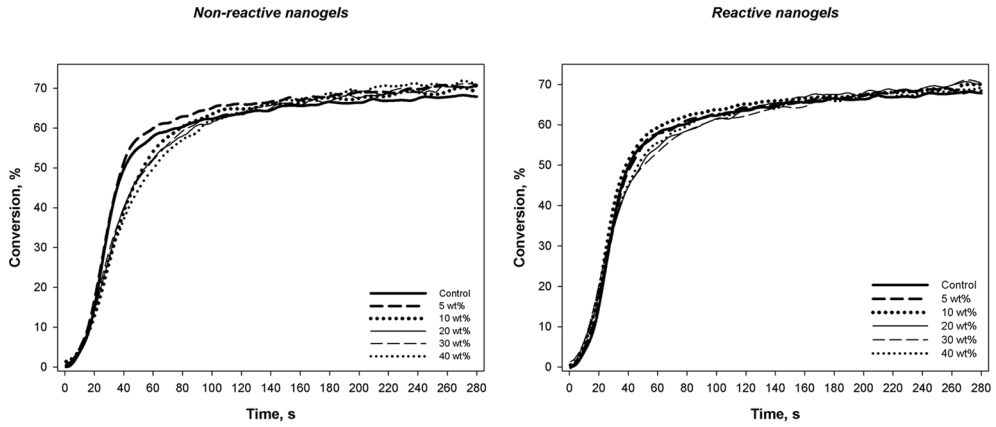

Figure 4.
Polymerization kinetics plots for TEGDMA with varied nanogel contents. Photopolymerizations were conducted with 320–500 nm light at an incident irradiance of 50 mW/cm^2.

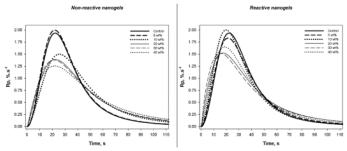

Figure 5.
Polymerization rate profiles.

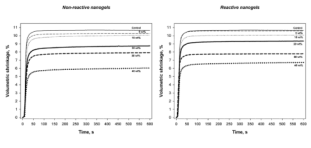

Figure 6.
Shrinkage kinetics of the resins.

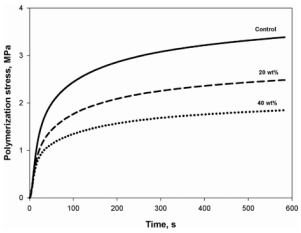

Figure 7.
Dynamic polymerization shrinkage stress profiles for TEGDMA monomer and the materials containing 20 and 40 wt% of reactive nanogel.

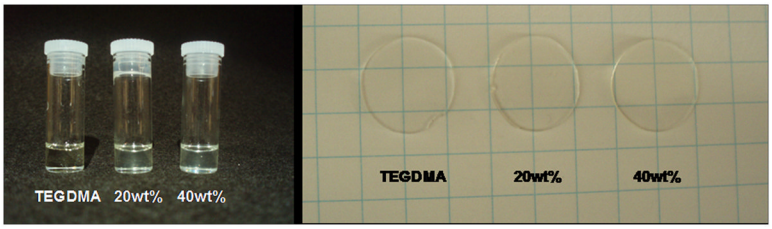

Figure 8.
Examples of the optical clarity of 0, 20 and 40 wt% nanogel-containing TEGDMA monomer and polymer samples.

Table 1

Nanogel effects on uncured monomer and composite properties

Nanogel fraction, wt%	Monomer viscosity, Pa.s*		Maximum filler loading, wt%	Slope of composite paste force/ displacement plot, N/mm#
	Non-reactive nanogel	Reactive nanogel		
0	0.0159 (0.001)^{d}		81.7	0.010 (0.006)^{c}
5	0.0164 (0.001)^{A,d}	0.0161 (0.003)^{A,d}	78.6	0.047 (0.010)^{c}
10	0.0206 (0.001)^{A,d}	0.0188 (0.002)^{A,d}	78.2	0.050 (0.008)^{c}
20	0.0497 (0.002)^{A,c}	0.0477 (0.004)^{A,c}	77.1	0.654 (0.071)^{c}
30	0.168 (0.003)^{A,b}	0.151 (0.002)^{A,b}	76.7	4.346 (0.163)^{b}
40	0.696 (0.003)^{A,a}	0.672 (0.003)^{A,a}	75.8	8.728 (0.901)^{a}

* Means with parenthetic standard deviation. Upper case letters indicate that there are no statistical differences in viscosity between analogous nanogel concentrations within a given row (paired t-test, α=5%). Lower case letters indicate statistical differences within a column (Tukey's test, α=5%).

Fitted linear force/displacement slope of 70 wt% barium glass filled composite paste.

Table 2

Means (standard deviations) for volumetric shrinkage (%)

Nanogel fraction, wt%	Resins*		Composites#
	Non-reactive nanogels	Reactive nanogels	
Control	10.66 (0.3)[a]		5.14 (0.2)[a]
5	10.27 (0.3)[A,a]	10.57 (0.4)[A,ab]	4.78 (0.1)[ab]
10	10.07 (0.5)[A,a]	10.07 (0.8)[A,ab]	4.51 (0.6)[b]
20	8.75 (0.4)[A,b]	9.35 (0.4)[A,b]	4.48 (0.3)[b]
30	7.92 (0.4)[A,b]	7.79 (0.1)[A,c]	4.61 (0.3)[b]
40	6.04 (0.2)[A,c]	6.72 (0.4)[A,c]	3.91 (0.04)[c]

*Means with parenthetic standard deviation. Upper case letters indicate that there are no statistical differences between analogous nanogel concentrations within a given row (paired t-test, α=5%). Lower case letters indicate statistical differences within a column (Tukey's test, α=5%).

#Composite formulations with fixed barium glass loading (70 wt%) and varied nanogel contents.

Table 3

Flexural strength (σ, MPa) and modulus (E_f, GPa) characterization of nanogel-modified TEGDMA resin and composite formulations

Nanogel fraction, wt%	Resin*				Composite#	
	Non-reactive nanogel		Reactive nanogel		Reactive nanogel	
	σ	E_f	σ	E_f	σ	E_f
0	111 (9)[a]	2.0 (0.2)[a]	111 (9)[a]	2.0 (0.2)[a]	124 (16)[a]	6.4 (1.7)[a]
5	120 (3)[a]	2.0 (0.1)[a]	113 (5)[a]	1.8 (0.1)[a]	141 (20)[a]	6.3 (0.8)[a]
10	118 (7)[a]	1.9 (0.1)[a]	109 (3)[a]	1.8 (0.1)[a]	130 (9)[a]	6.7 (0.4)[a]
20	89 (7)[b]	2.0 (0.1)[a]	109 (5)[a]	2.0 (0.1)[a]	115 (7)[a]	6.6 (0.5)[a]
30	62 (5)[c]	2.3 (0.2)[a]	103 (4)[a]	2.0 (0.1)[a]	120 (4)[a]	5.8 (0.9)[a]
40	43 (8)[d]	2.2 (0.3)[a]	104 (3)[a]	2.0 (0.1)[a]	117 (6)[a]	6.8 (0.7)[a]

*Means with parenthetic standard deviation. Lower case letters indicate statistical differences within a column (Tukey's test, α=5%).

#Composite formulations with fixed barium glass loading (70 wt%) and varied nanogel contents.

Dent Mater. Author manuscript; available in PMC 2012 June 1.

Table 4

Results for refractive index and translucency of the nanogel-modified resins

Nanogel fraction, wt%	Refractive index*		Relative optical clarity#	
	Non-Reactive	Reactive	Monomer	Polymer
0	1.4603		1.000 (0.003)^{A,a}	0.869 (0.003)^{B,a}
5	1.4628	1.4625	-	-
10	1.4655	1.4650	-	-
20	1.4711	1.4698	0.874 (0.006)^{A,b}	0.770 (0.002)^{B,b}
30	1.4749	1.4742	-	-
40	1.4823	1.4800	0.822 (0.005)^{A,c}	0.738 (0.003) ^{B,c}

*Refractive index at 23°C.

#Relative optical clarity as compared with unmodified TEGDMA monomer. Upper case letters indicate statistical differences between analogous nanogel concentrations within a row (paired t-test, α=5%). Lower case letters indicate statistical difference within a column (Tukey's test, α=5%).